absent because they should be able to form with equal probability. Therefore, the FT-IR studies seem to show that the CAN/CHD copolymerization results mainly in 1,4-linkages in the cyclohexene unit irrespective of the initiator or temperature of polymerization.

An extensive nuclear magnetic resonance study involving ^{1}H, 2D ^{1}H COSY, ^{13}C NMR, DEPT, and CSCM allowed a complete structural assignment and indicated that the methine protons are allyllic to the double bond in the cyclohexene unit. This is consistent with the copolymer containing essentially 1,4-linkage in the cylcohexene unit, though the absolute exclusion of 1,2-linkages is not possible. The peaks for the various types of carbons in the CAN/CHD copolymer were assigned with use of the DEPT spectrum of the above copolymer.

Acknowledgment. We wish to thank the IBM Instruments Division, Danbury, CT, for the 300-MHz ^{1}H and 75-MHz ^{13}C and DEPT NMR spectra of the poly(CAN/CHD). Expert assistance lent by John Harwood, James Cushman, and Charles Savage with the 2D NMR studies is greatly appreciated along with valuable comments on the interpretation of the 2D NMR results from one reviewer. The financial support given by the Center for Energy Conversion Research Power Conditioning Lab, University of Texas at Arlington, and a grant from the Defense Advanced Projects Agency, monitored by the Office of Naval Research is also gratefully acknowledged.

Registry No. (2-CAN)(1,3-CHD) (alternating copolymer), 110536-76-0.

References and Notes

(1) Cowie, J. M. G. *Alternating Copolymers*; Plenum: New York, 1985.
(2) Hirai, H. *J. Polym. Sci., Macromol. Rev.* **1976**, *11*, 47.
(3) Gaylord, N. G.; Stolka, M.; Patnaik, B. K. *J. Macromol. Sci., Chem.* **1972**, *A6*, 1435.
(4) Gaylord, N. G.; Maiti, S.; Patnaik, B. K.; Takahashi, A. *J. Macromol. Sci., Chem.* **1972**, *A6*, 1459.
(5) Gaylord, N. G.; Maiti, S.; Dixit, S. S. *J. Macromol. Sci., Chem.* **1972**, *A6*, 1521.
(6) Butler, G. B.; Badgett, J. T.; Sharabash, M. *J. Macromol. Sci., Chem.* **1970**, *A4*, 51.
(7) (a) Nagai, K.; Machida, S.; Nonaka, T. *J. Polym. Sci., Polym. Chem. Ed.* **1981**, *19*, 773. (b) Moore, J. A.; Partain, E. M. *J. Polym. Sci., Polym. Chem. Ed.* **1985**, *23*, 591.
(8) Marvel, C. S.; Hartzell, G. E. *J. Am. Chem. Soc.* **1959**, *81*, 448.
(9) (a) Ballard, D. G. H.; Courtis, A.; Shirley, I. M.; Taylor, S. C. *J. Chem. Soc., Chem. Commun.* **1983**, 954. (b) Ballard, D. G. H.; Courtis, A.; Shirley, I. M. Europer Patent Appl. 0 122 079 A2, 1984.
(10) McKean, D. R.; Stille, J. K. *Macromolecules* **1987**, *20*, 1787.
(11) Nagai, K.; Yamagai, Y. *Nippon Kagaku Kaishi* **1985**, *12*, 2310.
(12) Bruch, M. D.; Payne, W. G. *Macromolecules* **1986**, *19*, 2710 and references cited therein.
(13) Doddrell, D. M.; Pegg, D. T.; Bendall, M. R. *J. Magn. Reson.* **1982**, *48*, 323.
(14) Nagayama, K.; Kumar, A.; Wüthrich, K.; Ernst, R. R. *J. Magn. Reson.* **1980**, *40*, 321.
(15) Bendall, M. R.; Pegg, D. T.; Doddrell, D. M. *J. Magn. Reson.* **1981**, *45*, 8.
(16) Lefebvre, G.; Dawans, F. *J. Polym. Sci., Polym. Chem. Ed.* **1964**, *2*, 3277.
(17) Florjanczyk, Z.; Siudakiewicz, M. *J. Polym. Sci., Polym. Chem. Ed.* **1986**, *24*, 1849.
(18) The combined uses of ^{13}C NMR and attached proton test (APT) for the HCl elimination product of the copolymer showed three quaternary carbons (two olefinic and one cyano) and two olefinic methine carbons.
(19) Silverstein, R. M.; Bassler, G. C.; Morrill, T. C. Spectrometric Identification of Organic Compounds, 4th ed.; Wiley: New York, 1980.
(20) Heilmann, H.; Bonnier, J. M.; Delepine, M. *C.R. Hebd. Seances Acad. Sci.* **1959**, *4*, 2595.
(21) Bellamy, L. J. *Advances in Infrared Group Frequencies*; Methuen: Suffolk, 1968.
(22) Pouchert, C. J. *The Aldrich Library of Infrared Spectra*, 2nd ed.; Aldrich Chemical: Milwaukee, WI, pp 443-461, 969-997.
(23) Hahn, B.; Percec, V. *J. Polym. Sci., Polym. Chem. Ed.* **1987**, *25*, 783.
(24) Green, G. D.; Hall, H. K.; Mulvaney, J. E.; Noonan, J.; Williams, D. J. *Macromolecules* **1987**, *20*, 716.
(25) Levy, G. C.; Lichter, R. L.; Nelson, G. L. *Carbon-13 Nuclear Magnetic Resonance* Spectroscopy; Wiley: New York, 1980; pp 78, 160.
(26) Jo, Y. S.; Inoue, Y.; Chujo, P.; Saito, K.; Miyata, S. *Macromolecules* **1985**, *18*, 1850.
(27) Sharaby, Z.; Martan, M.; Jagur-Grodzinski, J. *Macromolecules* **1982**, *15*, 1167.
(28) Tonelli, A. E.; Schilling, F. C. *Acc. Chem. Res.* **1981**, *14*, 233.
(29) Mirau, P. A.; Bovey, F. A. *Macromolecules* **1986**, *19*, 210.
(30) Schilling, F. C.; Bovey, F. A.; Bruch, M. D.; Kozlowski, S. A. *Macromolecules* **1985**, *18*, 1418.

The Structure of Poly(D-(−)-β-hydroxybutyrate). A Refinement Based on the Rietveld Method

S. Brückner,* S. V. Meille, and L. Malpezzi

Dipartimento di Chimica del Politecnico, P.zza L.da Vinci 32, 20133 Milano, Italy

A. Cesàro, L. Navarini, and R. Tombolini

*Dipartimento di Biochimica, Biofisica e Chimica delle Macromolecole,
P.le Europa 1, 34127 Trieste, Italy.* *Received August 10, 1987*

ABSTRACT: The crystal structure of optically active microbial poly(D-(−)-β-hydroxybutyrate) has been refined with the Rietveld whole-fitting method applied to powder X-ray diffraction data. This natually occurring polymer gives rise to a very crystalline phase and therefore to very detailed and resolved powder profiles. Reliability of the refinement is discussed in relation to results obtained from previous studies on oriented-fiber diffraction patterns. The conclusion is that well-detailed powder profile data are highly discriminatory toward structural models not very dissimilar from each other. This result is considered an encouraging step toward a more general assessment of the accuracy of structural parameters obtained from best fitting of powder X-ray diffraction profiles.

Introduction

The structure of crystalline polymers can be determined or refined through best-fitting of X-ray powder diffraction profiles.[1,2] This technique, known as the Rietveld whole-fitting method,[3] is the only accessible X-ray diffraction approach when, for some reason, it is impossible to obtain oriented samples.

Some recent successful structure determinations, adopting this method,[1,2] raised the problem of what confidence should be attributed to the structural models one

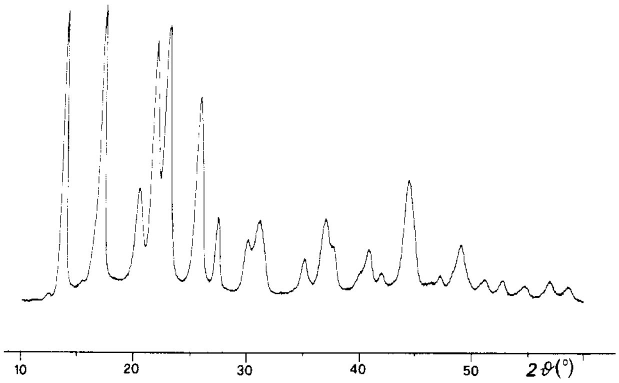

Figure 1. Powder X-ray diffraction profile of PHB.

can obtain, in particular when compared to the much more common determinations based on X-ray diffraction from oriented samples. An answer to this question cannot be straightforward since two contradictory features are to be taken into account and properly compared: (i) the monodimensional distribution of diffracted intensities with the consequently enhanced overlapping problems and (ii) the rigorously quantitative measurement of diffraction profiles followed by a comparison procedure where arbitrary assumptions are really kept to a minimum.

As a contribution to a more concrete feeling on these issues we decided to study a polymer whose crystal structure has been already extensively investigated through X-ray diffraction from oriented fibers. A particularly favorable example, from this point of view, is represented by poly(β-hydroxybutyrate) (hereafter referred to as PHB).

This optically active thermoplastic aliphatic polyester is produced and accumulated as a source of energy and carbon by a number of microorganisms.[4] Many years after the first physicochemical studies,[5] PHB is again attracting attention[6] because of its commercial interest. Furthermore, it has been shown that its natural production is more a rule than an exception in the microbial world and that other stereoregular polyesters with longer aliphatic side chains are also synthetized.

Among the many nonpathogenic microorganisms accumulating PHB, *Rhizobium* was chosen[7] as source because of its agricultural importance and for the extensive knowledge of its biochemistry, physiology, and ecology. The production, extraction and characterization procedures are described in the Experimental Section. What we want to stress here is the outstanding stereoregularity and crystallinity of this polymer giving rise to X-ray powder diffraction spectra very well detailed up to high 2θ values (see Figure 1).

To our knowledge two structural studies were carried out on PHB, both of them based on X-ray diffraction data from oriented fibers. One is due to Cornibert and Marchessault[8] (hereafter referred to as model I) and the other to Tadokoro and co-workers[9] (model II). It is worthwhile pointing out that these two studies were carried out following different criteria. Model II is the result of a least-squares procedure that optimizes the agreement between observed and calculated intensities by adjusting all internal coordinates of the chain, while model I was obtained, together with other possible conformers, by a preliminary conformational analysis. Agreement with diffracted intensities for model I was optimized by allowing only rigid-body refinement; it assumes therefore the meaning of a figure of merit to discriminate, among many conformers, the most likely to be present in the crystalline state. The two procedures provide results grossly in agreement with respect to the conformation of the chain in the crystal but differing significantly on a more detailed scale. For example, the ester bond is assumed rigorously trans in model I, while model II allows for a deviation of 5° from planarity. Such differences represent, in our opinion, an additional reason of interest in performing a new structural study based on a different approach.

Table I
Experimental Conditions of Profile Recording

instrument	Siemens D-500 goniometer equipped with step-scan attachment, proportional counter, and Soller slits, controlled with a Hewlett-Packard computer
radiatn (power)	Cu Kα, Ni-filtered (40 kV, 30 mA)
divergence aperture, deg	0.3
receiving aperture, deg	0.05
step width, deg	0.05 (2θ)
count time, s per step	40
2θ range, deg	10–60

Experimental Section

Polymer Production and Extraction. PHB was produced from *Rhizobium leguminosarum.* Cultural medium: Fiton (Becton, Dickinson BBL) 2.0 g/L, glucose 10.0 g/L, K_2HPO_4 0.5 g/L, $MgSO_4$ 0.2 g/L, autolyzed yeast 1.0 g/L, pH 7.2. Growth was made in a 750-mL Erlenmeyer flask with 100 mL of medium at 25 °C on a rotatory shaker at 100 rpm. PHB content was determined with the gas chromatographic method described by Braunegg et al.[10] The yield in PHB, after 4 days, was 2.8 g/L with a biomass (dry weight) of 5.9 g/L.

For the extraction of PHB the culture broth was centrifuged at 1000 rpm for 10 min (at 25 °C). Cell pellet was washed and suspended in distilled water and collected by centrifugation. Cells were suspended in acetone, which was removed by filtration, and the solid was then desiccated. The dried powder was suspended in chloroform (2 wt/vol % solution) at 30 °C, and water was added to extract hydrophilic material. After mild centrifugating, cell debris is packed at the interface and PHB remains in the organic phase. The polymer was precipitated with 2× volumes of cold acetone and washed with diethyl ether and water.

Polymer Characterization. Chemical Analysis. The chemical identity of the polyester extracted from *Rhizobium leguminosarum* was determined by ^{1}H NMR spectra of 1 wt % solutions of PHB in $CDCl_3$. Spectra were recorded at 60 MHz on a Varian EM360 NMR spectrometer (TMS internal standard). All data were in agreement with literature.[6b]

Viscometry. The average molecular weight of the sample was determined from viscosity measurements by using the Mark–Houwink relation[11] $[\eta] = 1.18 \times 10^{-4} M^{0.78}$, obtaining $M_v = 1.6 \times 10^6$. Intrinsic viscosity was evaluated on chloroform solutions with a Schott-Gerate AVS/G equipment with an Ubbelhode viscosimeter (i.d. = 0.46 mm), immersed in a thermostatic bath at 30 °C.

Thermal Analysis. Differential scanning calorimetric (DSC) measurements were done on a Dupont DSC-9900 calorimeter on samples of about 10 mg in a temperature range of 50–200 °C with a scan rate of 10 °C/min. Thermogravimetric (TG) measurements were performed on a Mettler Thermal Analyzer TA-2000 C, using Al_2O_3 as reference with a scan rate of 10 °C/min.

X-ray Diffraction. PHB, 150 mg, was used to fill the sample holder of a D-500 Siemens goniometer equipped with an Anton Paar temperature controller. Annealing was directly carried out in situ by raising the temperature of the sample holder to 170 °C for 15 min under vacuum conditions (≅0.001 mmHg). After spontaneous cooling (≅30 min) to room temperature a quantitative recording of the powder X-ray diffraction profile started under conditions described in Table I.

Structural Analysis

In order to identify the conditions for optimal annealing and processing, the thermal behavior of PHB was examined. On the sample used for X-ray diffraction ($M_v = 1.6 \times 10^6$) thermogravimetric results show remarkable stability up to 200 °C (see Figure 2). Thermograms of the dried

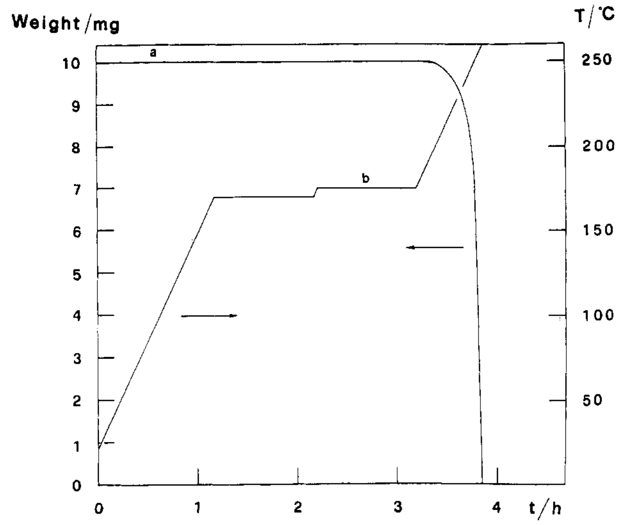

Figure 2. Plot of the thermogravimetric analysis carried out, under air flow (50 mL min^{-1}), as a function of time (curve a). The heating program is represented by curve b.

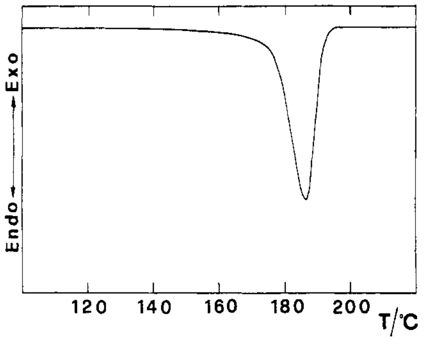

Figure 3. DSC plot of PHB heated and annealed as described in the text.

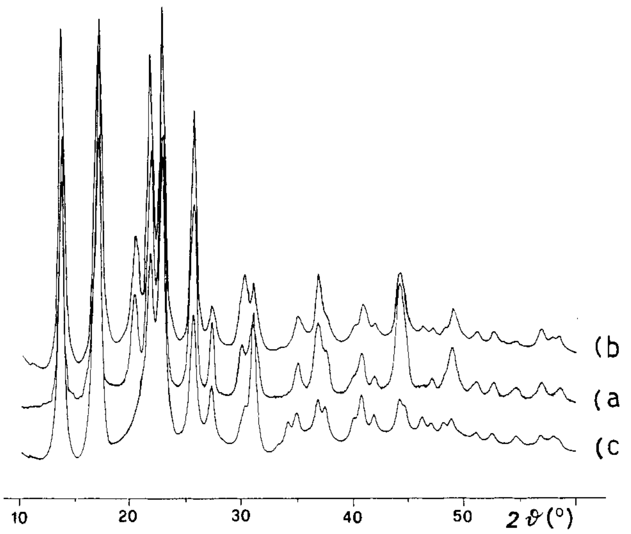

Figure 4. Comparison involving the experimental profile of PHB (curve a), the calculated profile for model I (curve c), and the calculated profile for model II (curve b).

Table II
Refined Cell Constants and Final Fractional Coordinates ($\times10^4$) of Model III

	x	y	z
O(1)	2899	177	4016
O(2)	-801	1078	-717
C(1)	4455	717	2513
C(2)	3032	1422	959
C(3)	1286	791	-387
C(4)	5902	1428	4032

[a] An isotropic thermal factor $B = 2.0$ Å^2 was assigned to each atom. $a = 5.73$ (1) Å; $b = 13.14$ (1) Å; $c = 5.93$ (1) Å; space group $P2_12_12_1$.

raw polymer show a broad melting peak at scan rate 10 °C/min,[7] with a T_m of 181 °C and $\Delta H_f = 93.0$ J/g. After the sample is annealed at 170 °C for 15 min, the heat of fusion increases to 112 J/g (T_m = 186 °C) (Figure 3).

Evaluation of the mass fraction of crystallinity from literature heat of fusion values[12] of PHB (146 J/g) affords a crystallinity fraction of 0.77. These results were deemed satisfactory and the sample for X-ray diffraction analysis was annealed accordingly.

The program used throughout our analysis was written by Immirzi[19] and modified by one of the authors in order to allow for the insertion of constraints among the generalized coordinates in the form of Lagrange multipliers.[14] Cell dimensions and space group (orthorhombic $P2_12_12_1$) were taken from published data, and only in the final optimization cycles were cell dimensions refined, only very modest changes resulting.

Models I and II were tested against the observed profile by performing a best-fitting refinement of all the following nonstructural parameters expected to have an influence on experimental data: (i) the background contribution (expressed in the form of a segmented line where the intensities at the selected nodes are adjustable quantities); (ii) the peak half-height widths and the 2θ dependence (quantities related to crystallites average dimensions and to lattice disorder or strains); (iii) the effect of uniaxial preferred orientation of crystallites that may be induced by manipulations of the sample as well as by surface effects that may occur during melting and subsequent annealing; (iv) an overall scale factor between calculated and observed data; and (v) a zero-correction to the experimental 2θ-scale. Peak profiles were always calculated analytically in the form of Cauchy functions[15] and Kα_1–Kα_2 splitting was taken into account.

Results of this test are reported in Figure 4, where curve a shows the experimental profile while curves b and c represent the best-fitting results for models II and I, respectively. The overall disagreement factors for the two models, in terms of $R = \sum|I_o - I_c|/\sum I_{net}$ (where $I_{net} = I_o - I_{backgr}$), are 0.341 and 0.200 for models I and II, respectively. In the last refinement cycles the weight attributed to the two peaks at low 2θ values (13.5° and 16.4°) was reduced to $0.1w$. The intensity of the latter peaks is substantially reproduced by both models, but owing to the low absorption of the material, they are affected by appreciable aberrations that produce a marked dissimmetry[16] so that an accurate fitting of the whole peak shape is difficult.

This preliminary test on models I and II was followed by a refinement procedure extended to structural parameters too. Model II was first chosen as the starting point and after few cycles of preliminary rigid-body adjustments the chain flexibility was increased by allowing all four torsion angles to vary. One bond length and two valence angles involving atoms that belong to adjacent cells were constrained, so that boundary conditions were fulfilled throughout the best-fitting procedure. Valence angles were also refined in the final stage while hydrogen atoms were located at calculated positions. In this case too, a reduced weight ($0.1w$) was attributed to the two peaks at low 2θ. The resulting refined model (model III) showed an overall disagreement factor R of 0.149 and its uniqueness was confirmed by performing a second refinement procedure that started from model I and led to a structure virtually undistinguishable from model III. In Table II we report

Table III
Valence and Torsion Angles of Model III[a]

Valence Angles, Deg			
O(1)–C(1)–C(2)	109.5 (10)	C(2)–C(3)–O(1)′	113.8 (10)
O(1)–C(1)–C(4)	106.0 (12)	C(2)–C(3)–O(2)	122.5 (13)
C(2)–C(1)–C(4)	106.0 (12)	O(1)′–C(3)–O(2)	123.7 (12)
C(1)–C(2)–C(3)	109.5 (10)	C(1)–O(1)–C(3)′	113.0 (11)
Torsion Angles, Deg			
C(3)′–O(1)–C(1)–C(2)	149 (2)	C(1)–C(2)–C(3)–O(1)′	–35 (2)
O(1)–C(1)–C(2)–C(3)	–59 (2)	C(2)–C(3)–O(1)′–C(1)′	–173 (2)

[a] For the numbering scheme of atoms see Figure 5.

Table IV
Refined Nonstructural Parameters

zero correction (2θ), deg	–0.108 (4)
preferred orientatn[a]	$G = 0.056$ (9); indices [001]
profile function param[b]	
U	0
V	0
W	0.375 (5)
m	1

2θ, deg	intensity[c]	2θ, deg	intensity[c]
10	0.310 (6)	26	0.330 (6)
12	0.200 (5)	36	0.410 (5)
15	0.210 (5)	42	0.515 (5)
18	0.295 (6)	52	0.460 (4)
22	0.200 (4)	60	0.370 (4)

[a] Preferred orientation factor PO = $\exp(-G\alpha_k^2)$, α_k is the angle between the scattering vector of the kth reflection and the scattering vector of a fixed (preferred) reflection. [b] Peak shapes are calculated analytically through a Pearson VII function $f(z) = (C/H_k)\,[1 + 4(2^{1/m} - 1)z^2]^{-m}$ with $z = (2\theta_i - 2\theta_k)/H_k$; $H_k^2 = U \tan^2 \theta_k + V \tan \theta_k + W$; $m = 1$ determines a peak profile following a Cauchy distribution. [c] Intensities (k counts) of the points on the segmented line.

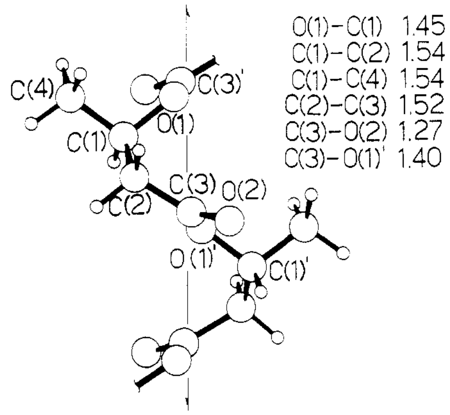

Figure 5. View of the polymer chain (model III) orthogonal to the chain axis. We also show the atom numbering scheme and the bond lengths (not refined).

the final fractional coordinates of model III, in Table III valence angles and torsion angles are listed, and in Table IV the refined nonstructural parameters are summarized. In Figure 5 we show a perspective view of the chain with the atom numbering scheme and bond lengths (not refined). A comparison between the observed (curve a) and calculated (curve b) profiles is shown in Figure 6 together with the background line (dashed line) and the difference profile (curve c). The calculated base line allows an evaluation of the crystallinity fraction of about 84%, not much higher than the 77% estimated from DSC measurements.[12]

Isotropic thermal parameters $B = 2.0$ Å^2 were adopted for nonhydrogen atoms throughout our calculations. This is an abnormally low value if compared with the 4–7 Å^2 usually adopted in this kind of structures analyzed at room temperature. Lowering thermal factors seems, however, to be a systematic tendency connected with the present approach; in fact we already adopted abnormally low thermal parameters in previous structures solved or refined from powder X-ray diffraction data.[1,2,17] The scarce physical meaning of such low thermal factors suggests that they are adopted as a mathematical device in order to account for some effect of different nature, probably an absorption effect.

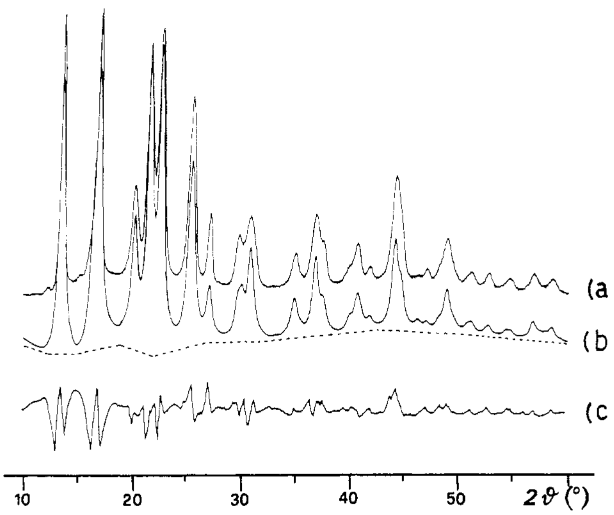

Figure 6. Comparison between the experimental profile of PHB (curve a) and the calculated profile for model III. Also reported are the calculated base line (dashed line) and the difference profile (curve c).

Discussion

Before discussing details of the structure analysis we want to point out that access to available models[8,9] has greatly simplified our work, but this is not a mandatory condition for the present approach to be applied. In fact in previous works[1,2,17] cell parameters and space group were determined without "a priori" information through a trial and error procedure while packing and conformational energy calculations were very helpful in defining the starting point for the refinement procedure.

Figure 4 shows how discriminatory a detailed powder profile can be. Model I, only weakly related to experimental data, and model II, obtained through an optimization based on diffracted intensities, show markedly different agreements with the observed profile. We recall here the disagreement factors R of 0.34 and 0.20 for model I and II, respectively. The most striking discrepancies are detected on curve c; in particular the observed peak at $2\theta = 20.2°$ (0 2 1) is practically ignored by model I, the peak at $2\theta = 30.9°$ (0 1 2) is highly overestimated, and the peak at $2\theta = 44.1°$ (1 4 2; 0 6 1) is calculated as rather weak in comparison with a rather strong observed intensity.

Curve b shows a substantial agreement with the observed profile on the whole 2θ range, even if some local discrepancies appear more severe than those allowable for a refined structure; in particular the calculated peak at $2\theta = 44.1°$ is still sensibly weaker than the observed one. In Figure 6 it may be seen that model III provides for a significant improvement through modest changes of the molecular geometry.

The comparison of model II and III is of particular interest, in our opinion, since they both result from a best-fitting procedure performed on experimental data and involving adjustments of internal coordinates. When the results obtained from the structure factors calculation of model III are compared with the set of observed data

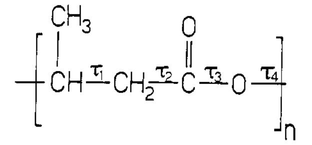

	model I	model II	model III
τ_1	-57	-52	-59
τ_2	-31	-42	-35
τ_3	180	-175	-173
τ_4	142	152	149

Figure 7. Four main-chain torsion angles of PHB for models I, II, and III summarized and compared.

reported in ref 9, a disagreement factor of 0.22 is obtained. Our refined model shows thus a worse agreement than model II (disagreement factor 0.15) when experimental data of ref 9 are taken into account. At this point an important remark is in order. In model III a length of 1.54 Å is assumed for the C–CH_3 bond while in model II the same bond is 1.62 Å long. The only reason for adopting, in that approach, a bond length of such low physical significance is that this was probably the only way to increase significantly agreement with observed data. We do not believe that the worsening from 0.15 to 0.22 above discussed for model III can be totally ascribed to this bond length, but this feature undoubtedly determines a sensible departure from those observed data. For what concerns more specifically the structural features of PHB, our study strongly supports the conclusion, already present in model II, that the ester bond deviates significantly from planarity (torsion angle = −173°). An even stronger deviation from planarity is required to interpret lanthanide-induced chemical shifts in chloroform solutions.[5b] Figure 7 reports a comparison among the main-chain torsion angles in the three models of PHB. Since models II and III are the best results obtainable from the two experimental data sets, we must conclude that their geometrical differences (see Figure 7) are a direct consequence of different evaluations of diffracted intensities; they represent therefore the order of magnitude of the *real* uncertainty affecting main-chain torsions in this polymer. Some of these differences are larger than the computed esd's, thus indicating the presence of systematic errors in the evaluation of experimental data and in the models adopted for their interpretation. For what concerns the Rietveld method applied to polymer structures, an important source of uncertainty is surely represented by the contribution from noncrystalline phases to powder diffraction profiles, and further difficulties may arise from the preferred orientation of crystallites. This problem is usually dealt with by assuming a uniaxial distribution of orientations around a given direction, but the real situation could present a more complicated texturing, with a sensible contribution to systematic errors in the treatment of diffracted intensities.

Traditional methods for evaluating integrated intensities in X-ray diffraction patterns from oriented samples involve also some uncertainty. The measurement of local intensity, its correction through proper spot-shape factors, and the background estimate are subject to errors due to the approximations involved. The resulting uncertainties are well testified by simply comparing observed data reported in ref 8 with those reported in ref 9. A disagreement factor can be computed through a one-by-one comparison *of the square roots of observed intensities* obtaining a disagreement factor of ≅10% on equatorial peaks and of ≅20% on layer peaks. Such discrepancies are really hardly detectable among powder diagrams unless marked texturing is present.

The recent introduction of two-dimensional scanning microdensitometers has indeed made it feasible to utilize far more of the information contained in the pattern directly, thus reducing the need for approximations and subjective decisions.[18] This is achieved, however, at the cost of heavy computational procedures handling a high number of data points (on the order of 10^6).

The comparisons carried out in this work are useful, in our opinion, because they point out that a well-detailed powder profile can be highly discriminatory toward structural models that show only modest conformational differences; this means that geometrical parameters resulting from a Rietveld analysis carried out on such experimental data are well defined within rather narrow limits. In fact the improvement of the disagreement factor for model III (R = 0.149) with respect to model I (R = 0.34) and model II (R = 0.20) occurs, as already stated, as a consequence of rather modest changes of torsion angles. If we consider that, for some torsion angles, model III is, roughly speaking, inbetween models I and II, we get an idea of the steepness of the minimum with respect to torsion angle changes. Moreover, an indication that this minimum is unique comes from having obtained the same refined structure starting from different models.

We acknowledge that any generalization should be carefully inferred; nevertheless we consider this conclusion as an encouraging indication of the substantial reliablity of structural results obtained through an approach that involves both ease of data collection and substantial simplicity of their elaboration.

Acknowledgment. This work has been supported by Ministero della Pubblica Istruzlone (MPI). R.T. is a recipient of a fellowship of Accademia dei Lincei, Rome, sponsored by Dutral S.p.A.

Registry No. PHB (SRU), 31759-58-7; PHB (homopolymer), 29435-48-1.

References and Notes

(1) Brückner, S.; Di Silvestro, G.; Porzio, W. *Macromolecules* **1986**, *19*, 235.

(2) Brückner, S.; Luzzati, S.; Porzio, W.; Sozzani, P. *Macromoleculs* **1987**, *20*, 585.

(3) Rietveld, H. M. *Acta Crystallogr.* **1967**, *22*, 151. Rietveld, H. M. *J. Appl. Crystallogr.* **1969**, *2*, 65.

(4) Lundgren, D. G.; Alper, R.; Schnaitman, C.; Marchessault, R. H. *J. Bacteriol.* **1965**, *89*, 245. Stockdale, H.; Ribbons, D. W.; Dawes, A. *J. Bacteriol.* **1968**, *95*, 1798.

(5) (a) Marchessault, R. H.; Okamura, K.; Su, C. J. *Macromolecules* **1970**, *3*, 735. Cornibert, J.; Marchessault, R. H.; Benoit, H.; Weill, G. *Macromolecules* **1970**, *3*, 741. Delsarte, J.; Weill, G. *Macromolecules* **1974**, *7*, 450. Okamura, K.; Marchessault, R. H. In *Conformation of Biopolymers*; Ramachandran, Ed.; Academic: London & New York, 1974; pp 709–720. (b) Delsarte, J.; Weill, G. *J. Phys.* (*Les Ulis, Fr.*) **1973**, *8*, 49.

(6) (a) Morikawa, H.; Marchessault, R. H. *Can. J. Chem.* **1981**, *59*, 2306. Marchessault, R. H.; Coulombe, S.; Morikava, H.; Okamura, K.; Revol, J. F. *Can. J. Chem.* **1981**, *59*, 38. (b) Doi, Y.; Kunioka, M.; Nakamura, Y.; Soga, K. *Macromolecules* **1986**, *19*, 1274.

(7) Scandola, M.; Pizzoli, M.; Ceccorulli, G.; Cesàro, A.; Paoletti, S.; Navarini, L., in preparation.

(8) Cornibert, J.; Marchessault, R. H. *J. Mol. Biol.* **1972**, *71*, 735.

(9) Yokouchi, M.; Chatani, Y.; Tadokoro, H.; Teranishi, K.; Tani, H. *Polymer* **1973**, *14*, 267.

(10) Braunegg, G.; Sonnleitner, B.; Lafferty, R. M. *Eur. J. Appl. Microbiol. Biotchnol.* **1978**, *2*, 29.

(11) Akita, S.; Einaga, Y.; Miyaki, Y.; Fujita, H. *Macromolecules* **1976**, *9*, 774.

(12) Barham, P. J.; Keller, A.; Otun, E. L.; Holmes, P. A. *J. Mater. Sci.* **1984**, *19*, 2781.

(13) Immirzi, A. *Acta Crystallogr., Sect. B* **1980**, *B36*, 2378.
(14) See, e. g.: Tadokoro, H. In *Structure of Crystalline Polymers*; Wiley: New York, 1979.
(15) Hall, M. M., Jr. *J. Appl. Crystallogr.* **1977**, *10*, 66.
(16) Klug, H. P.; Alexander, L. E. In *X-ray Diffraction Procedures*; Wiley: New York, 1974.
(17) Brückner, S.; Porzio, W. *Makromol. Chem.*, in press.
(18) French, A. D., Gardner, K. H., Eds. *Fiber Diffraction Methods*; ACS Symposium Series 141; Americal Chemical Society: Washington, DC, 1980. Symposium on Polymer Diffraction, Philadelphia, 1984: *J. Macromol. Sci., Phys.* **1985–1986**, *B24*, 1–4.

Solvent Dependence of Energy Trapping in Methacrylic Acid–Vinylphenanthrene Block Copolymers

Keiko Kamioka and S. E. Webber*

Department of Chemistry and Center for Polymer Research, University of Texas at Austin, Austin, Texas 78712

Yotaro Morishima

Department of Macromolecular Science, Faculty of Science, Osaka University, Toyonaka, Osaka 560, Japan. *Received July 8, 1987*

ABSTRACT: Steady-state and time-dependent fluorescence studies have been carried out on A–B–A block copolymers in which A = methacrylic acid and B = 9-vinylphenanthrene. The length of the B block greatly modifies the fluorescence properties of the polymer, especially in poorer solvents. In particular energy trapping at a weakly bound excimer site increases along the solvent sequence DMF, DMF/methanol, methanol. For a given solvent the energy trapping increases in the order of the degree of polymerization of the vinylphenanthrene sequence. A simple coil simulation lattice model with excitation random walk was studied in order to understand the experimental results on a molecular level. While the model is crude, it implies that the time-dependent fluorescence is most dependent on density of traps and the excitation transfer time and weakly dependent on the number of intracoil contacts.

Introduction

The study of photophysical processes of polymers with pendent aromatic chromophores has been quite active in recent years. In general these are complex systems with a wide range of local conformations of neighboring groups, energy trapping via excimer formation, and down-chain energy transfer. In the present paper we report the results of detailed fluorescence studies of methacrylic acid (MA) (A)–9-vinylphenanthrene (VPh) (B) A–B–A block copolymers (1) which have been studied previously by Morishima et al.[1] Our objective is to elucidate the relationship between the nature of a solvent and the extent of energy trapping and energy transfer within the phenanthrene blocks. In particular we attempt to ascertain if cross-chain energy migration occurs in this system by comparing our photophysical studies with a simple lattice model of the polymer chain. We carry out this comparison by using a "fractal" expression for the fluorescence decay function

$$I(t) = \exp(-at^{\tilde{d}/2} + bt^{\tilde{d}} - t/\tau_0) \qquad (1)$$

in which $\tilde{d}$ is the so-called "spectral" dimension and τ_0 is the unperturbed lifetime of the chromophore. This expression is based on a random walk to traps distributed on a lattice.[2] The spectral dimension may vary between 1 (ideal 1-D) and 2 (ideal 3-D). For the case of a phenanthrene block of ca. 43 units we find $\tilde{d}$ to vary from 1.08 to 1.4 as the solvent is changed from DMF (good solvent for the phenanthrene) to methanol (poor solvent for the phenanthrene). This variation is consistent with the idea that the phenanthrene block undergoes a transition from a random coil to a compact coil of higher effective dimensionality (e.g. significant numbers of non-nearest-neighbor phenanthrene contacts).

Table I
Degree of Polymerization of Block Copolymer

sample	DP_{MA}–DP_{VPh}–DP_{MA}
B-VPh-43	77–43–77
B-VPh-16	53–16–53
B-VPh-7	23–7–23
R-VPh-21[a]	

[a] Random copolymer of VPh and MA (Ph content 21 mol %).

Although monomeric phenanthrene does not form excimers in concentrated solution, phenanthrene groups tethered together on short chains[3] or pendent to polymer chains[4] have been reported to exhibit an excimer-like fluorescence which is less red-shifted relative to that of the monomer than for many other "classical" aromatic excimers (e.g. naphthalene, pyrene). We find the same type of fluorescence feature in the present experiments, the intensity of which is solvent-dependent. We assign this solvent dependence to the density of excimer forming sites (efs). It is these sites that we believe act as traps for the mobile monomeric excitation. Thus the solvent quality is thought to modify the effective dimensionality of energy migration and the density of the efs. It is not possible at present to deconvolute uniquely these two effects. One complication is that the efficiency of populating the excimer as measured by steady-state spectroscopy is higher than measured by the monomer lifetime shortening. This situation is normally referred to as "static quenching", which means simply that there exists a sensitization process that is faster than can be measured in the fluorescence decay.

Experimental Section

(a) Materials. MA–VPh–MA block copolymers and a VPh–MA random copolymer were prepared by Y. Morishima et al. at Department of Macromolecular Science, Osaka University, Osaka, Japan.[1] Table I lists the block and random copolymer samples used in the present study.

N,*N*-Dimethylformamide (DMF) was purified by fractional distillation. Methanol (Fisher Scientific Certified A.C.S. Spectranalyzed) was used as received. All solutions used for

0024-9297/88/2221-0972$01.50/0